

Cascades of Nuclear Disintegrations Induced by the Cosmic Radiation*

G. COCCONI, V. COCCONI TONGIORGI, AND M. WIDGOTT
Laboratory of Nuclear Studies, Cornell University, Ithaca, New York

(Received April 3, 1950)

Energetic nuclear disintegrations induced by the N -component of the cosmic radiation have been studied by detection of the moderate energy neutrons released in the disintegrations themselves.

The pulses of the neutron counters appeared on the sweep of a cathode-ray tube. A hodoscope of neon bulbs connected to an arrangement of G-M counters was simultaneously used to study the relative number of neutral and charged primaries and the penetration of the ionizing particles produced in the disintegrations.

Lifetime, angular distribution, and average energy of the neutrons have been investigated. The multiplicities of the neutrons produced in absorbers of different thickness and material have been determined. Evidence has been derived of the existence of conspicuous cascades of nuclear disintegrations.

A tentative analysis of the nuclear cascade process is given.

I. INTRODUCTION

IT has recently become more and more evident that in energetic nuclear interactions particles can be produced which are capable of inducing further nuclear processes, hence of causing a cascade-like development of nuclear events. This has been borne out principally by the analysis of cloud-chamber pictures and of photographic plates in which successive correlated events were recorded.

The experiment we are going to describe is an attempt at obtaining quantitative information about the nuclear cascade process by using the neutrons released in the nuclear disintegrations as indicators of the disintegrations themselves. The justification of this method can be found in the following arguments.

The interpretation of stars of heavily ionizing particles as nuclear evaporations implies the assumption that neutrons of moderate energies¹ are emitted from the excited nuclei along with the ionizing particles observed in these low energy events.

The fact that moderate energy neutrons have been recorded in coincidence with penetrating showers,² as well as the fact that many cloud-chamber pictures of penetrating showers show heavily ionizing tracks either at the origin or in the development of the showers, indicates that neutrons of moderate energies are boiled off from the nuclei also when high energy events take place.

Since electron sensitive plates have been introduced to study nuclear events, practically all nuclear disintegrations showing showers of particles at minimum ionization have been found to be accompanied by heavily ionizing particles.³

The experimental evidence finds easy interpretation as high energy interactions are expected to leave the nucleus generally in an excited state. The neutrons of

moderate energy and the charged particles capable of crossing the potential barrier are then the products of evaporation of the excited nucleus, hence the by-products of the main reaction among the fast particles.

These arguments lead one to infer that *all nuclear disintegrations induced by the cosmic radiation, whatever the energy involved in the process, release a number of neutrons of moderate energies, produced by nuclear evaporation. If a nuclear cascade occurs, neutrons of moderate energy are produced in each step of its development.*

The method has two main advantages.

(1) It can give information about the development of the nuclear processes *inside the detector* as the neutrons produced both in the primary and in secondary events have a large probability of emerging from the absorber. This is due to the fact that the absorbers commonly used, Pb, Al, and C, have very small cross sections for neutron capture.

(2) It allows the selection of nuclear events in a rather unbiased manner. In fact, the average energy and the angular distribution of the neutrons released in nuclear evaporations probably do not depend strongly on the energy and the nature of the process that excited the nucleus. The number of neutrons released will depend on these factors and a variation in neutron multiplicity will cause a variation in the probability of recording the events. However, this bias is removed by the possibility of determining the probability of recording all events as a function of the number of neutrons produced. This is not easily possible when detecting events by means of the charged products of the disintegrations.

The detection of nuclear disintegrations through the neutrons released in them has the disadvantage that the efficiency for neutron detection is necessarily small. However, this trouble is overcome in part, at least in absorbers of high atomic number, by the fact that the neutrons are produced with a rather high multiplicity.

II. EXPERIMENTAL

The experiment was performed at Echo Lake, Colorado (3260 m altitude, 708 g/cm² average pressure), during the summer of 1949.

The arrangement used is sketched in Fig. 1. Trays a , b , c , and d consisted of G-M counters, whereas trays A , B , C , and D consisted of BF₃ proportional counters.

The events studied were those occurring in the absorber Σ ; the absorber S was used in part of the ex-

* The cost of instrumentation of this work was supported by the ONR.

¹ We shall call "neutrons of moderate energy" the particles with energies between about 0.5 and 50 Mev. Particles having energies above 50 Mev will be called "high energy," or "fast" neutrons.

² Cocconi, Tongiorgi, and Greisen, *Phys. Rev.* **74**, 1867 (1948).

³ See, e.g., Kaplon, Peters, and Bradt, *Phys. Rev.* **76**, 1735 (1949).

periment to study the penetration of the ionizing particles produced in the nuclear disintegrations.

The large paraffin block ($38 \times 26 \times 26$ in.) in which the BF_3 counters were embedded served the purpose of slowing the neutrons of moderate energy down to thermal energies.

Trays *a*, *c*, and *d* consisted, respectively, of 23, 20, and 20 G-M counters, each of 1×16 in. effective surface. Tray *b* consisted of 24 G-M counters, each $\frac{1}{2} \times 10$ in. The solid angle defined by trays *b* and *c* was mostly covered by the counters in tray *a*.

Three G-M counters, *s*, each 2×40 in., were located around the system at the vertices of a triangle of 3-m sides and were used as monitors for extensive showers. They facilitated the selection of the events associated with extensive showers of high local density, which were disregarded.

The BF_3 proportional counters in *A* and *D* had 1×20 in. effective area; those in *B* and *C* were somewhat shorter (1×18 in.). All of them were filled with BF_3 (96 percent B^{10}) at 1.5 atmos. They were constructed and operated as described in a previous paper.⁴

In the course of the experiment data were taken with the neutron counters connected in two ways: In one, which we shall call hereafter "up-down connection," the 10 counters *A* and *B* were connected in parallel and their pulses fed into an amplifier, N_1 . A second amplifier, N_2 , was connected to the counters *C* and *D* similarly connected in parallel. In the other case, which we shall call "close-far connection," the 10 counters *B* and *C* were connected in parallel and their pulses fed into the amplifier N_1 , whereas the pulses of *A* and *D* were fed into N_2 .

A master pulse, *MP*, was generated whenever a coincidence between trays *b* and *c* was accompanied by at least one pulse in any of the 20 BF_3 counters, occurring between 5 and 15 μsec . after the coincidence *bc* happened ($MP = bc, N$). This was realized by shaping the coincidences (*b, c*) in a 10- μsec . square pulse, delayed 5 μsec . The delay was introduced to remove the possibility of spurious *MP*'s due to pulses in the BF_3 counters caused by particles different from neutrons, released in the disintegration itself (slow protons, bursts of electrons, etc.).

The frequency of *MP*'s due to chance coincidences has been evaluated as about 4 hr^{-1} , while the frequencies of the recorded events ranged between 13 and 70 hr^{-1} , depending on the thickness and nature of the absorber.

The requirement of the coincidence (*bc, N*) implies the presence of at least one ionizing particle emerging from the absorber, capable of crossing at least 22 g/cm^2 of paraffin (minimum energy for a proton ~ 170 Mev, for a meson ~ 75 Mev). This rules out a large number of events of low energy and makes our system sensitive to rather energetic nuclear interactions, with very little

requirement about angular distribution and number of ionizing particles produced in these.

We think that no important fraction of the recorded events, chance coincidences subtracted, can be due to known processes other than the nuclear interactions which we intended to study. In fact, no contribution can arise from the capture in the absorber of negative μ -mesons, as no penetrating ionizing particles are emitted in such a process along with the neutrons. Spurious events could be produced by neutrons generated by photons through (γ, n) reactions, if associated ionizing particles capable of producing a coincidence (*b, c*) are also present. This may be the case, when a μ -meson gives rise to a burst in the absorber Σ . Levinger⁵ has calculated that a photon of 10^{10} ev completely absorbed in lead can produce, on the average, about two neutrons. The rate of bursts of energies greater than 10^{10} ev produced in the thickest absorber Σ we used ($4\frac{1}{2}$ -in. Pb, surface 1160 cm^2) can be expected to be around 0.2 hr^{-1} , on the basis of results by Hudson.⁶ As the rate of the events recorded with the same absorber is ~ 55 hr^{-1} , the contribution due to meson bursts is negligible. Also small, in our opinion, is the background due to cascades produced by incident electrons and photons. In fact, only electrons and photons of very high energies have an appreciable probability of giving rise to an event capable of generating a *MP*. These are very rare, and they will probably fall on the apparatus accompanied by other electrons, in which case the events will be classified as due to "air showers," hence disregarded. It is, finally, important to point out that if an appreciable background is due to events of the kinds listed above, it must be confined essentially to the category of pictures showing a single neutron pulse, which have been disregarded in most of the discussions presented in this paper.

Whenever a *MP* occurred, a camera was triggered which took a picture of the following objects:

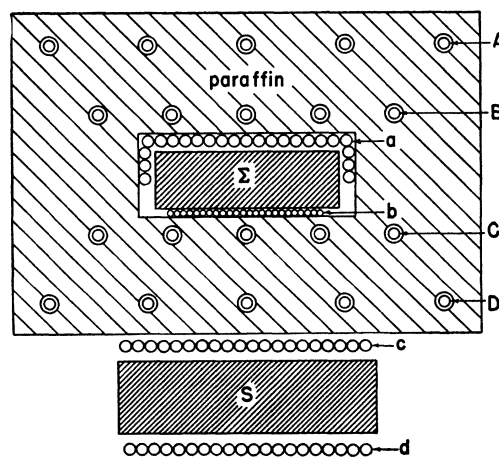


FIG. 1. Experimental arrangement.

⁴ V. Cocconi Tongiorgi, Phys. Rev. **75**, 1532 (1949).

⁵ J. Levinger, Nucleonics **6**, No. 5, 64 (1950).

⁶ D. Hudson, thesis, Cornell University.

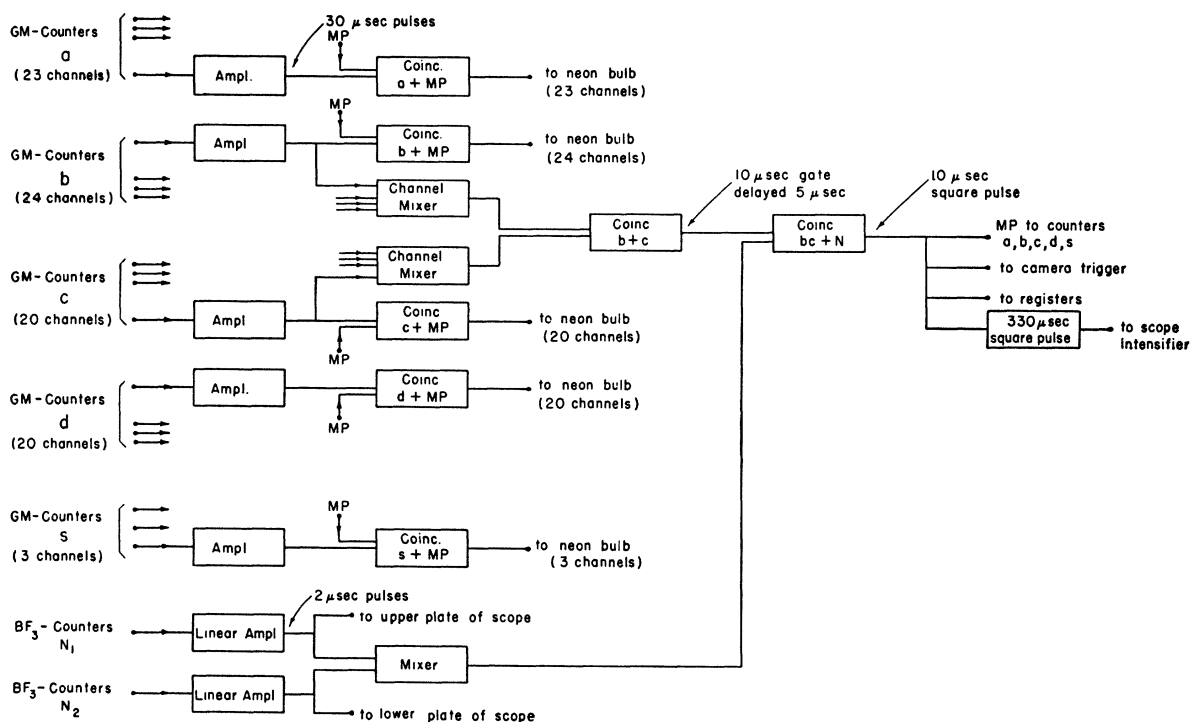


FIG. 2. Block diagram of the circuit.

(a) a mechanical register which numbered the pictures, and worked in parallel with another register located outside the camera box,

(b) a hodoscope of neon bulbs, each connected to one of the 90 G-M counters in trays *a*, *b*, *c*, *d*, and *s*, through a circuit that lighted the neon bulbs only when a pulse from the individual counter was followed within 30 μsec. by a *MP*;

(c) a five-in. cathode-ray tube (5RP-11, 5000 v accelerating potential), in which a linear sweep 330 μsec. long was started by the *MP*. To improve the time resolution, the path of the sweep followed eight horizontal saw teeth, each 40 μsec. long, vertically displaced from one another. The upper deflecting plate of the CRT was connected to the output of the neutron pulse amplifier *N*₁, and the lower plate to the output of *N*₂. Hence the neutron pulses (2 μsec. wide) appeared on the sweep as positive or negative pulses, depending on whether they were coming from amplifiers *N*₁ or *N*₂. We have therefore been able to establish, for each event, how many neutron pulses occurred in the BF₃ counters and with what delay each of them followed the first neutron pulse, which created the *MP*. The resolution in time of the pulses on the sweep, essentially determined by the amplifier, was about 1 μsec. It is worth pointing out that the occurrence of a pulse in one of the neutron counters does not affect the ability of the same counter to record other neutrons, since proportional counters have no deadtime, and the different pulses due to slowed-down neutrons are not likely to be simultaneous.

A block diagram of the circuit is given in Fig. 2.

Examples of the pictures obtained are presented in Figs. 3(a) and 4(a). These pictures are taken from the series of measurements made with $\Sigma=4\frac{1}{2}$ -in. Pb and $S=0$. The BF₃ counters were in the up-down connection.

In the course of the experiment, approximately 30,000 pictures were taken. Each of these has been transferred to a card, as shown by the examples given in Figs. 3(b) and 4(b).

It is obvious that the neutrons observed are not all of the neutrons created in the interactions, but only those which our neutron detector, with its limited efficiency, could record. Our detector is sensitive to neutrons with energies between ~ 1 and ~ 15 Mev. In this energy range, its efficiency, E , for recording a neutron is given by:

$$E = \eta \cdot \alpha \cdot (\omega/4\pi) \cdot k,$$

where η is the probability that a thermal neutron entering a counter gives rise there to a pulse; α is the probability that a neutron is slowed down to thermal energies in the neighborhood of the counters and enters one of them; $\omega/4\pi$ is the probability that a neutron is produced in the useful solid angle (with the assumption of isotropic distribution of the neutrons emerging from Σ , see Section IV) and k is the probability that the pulse from the neutron counter occurs within the time interval determined by the circuit.

We have estimated $\eta \approx 0.3$, $\omega/4\pi \approx 0.8$, $\alpha \approx 0.15$ for neutrons of energies between 1 and 15 Mev and our

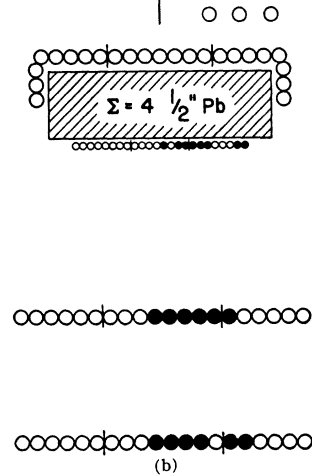
FIG. 3. Example of a picture (a) and a card (b) of a shower probably produced by a neutral primary. One neutron is required to trigger the sweep of the CRT, 7 neutron pulses are visible on the sweep. No neon bulbs are lit in columns 1, 2, and 3 of the hodoscope, which are connected to the counters in tray *a*. The bulbs in columns 4, 8, and 12 are always lit to provide fiducial marks. The bulbs in column 5, 6, and 7 are connected to tray *b*; 9, 10, and 11 to tray *c*; and 13, 14, and 15 to tray *d*.



(a)

TOTAL NUMBER OF NEUTRONS: 8

UP	DOWN
16 μ sec	69 μ sec
27	113
43	185
238	



20 BF_3 counters, hence in our apparatus we have $\eta \cdot \alpha \cdot \omega / 4\pi \approx 0.04$. An experimental determination of this product has been made by measuring the counts produced in our BF_3 counter arrangement by a calibrated 1 mC (Ra+Be) neutron source. The result was 0.037. The fair agreement with our estimate must be taken with the reservation that the energy spectra of the neutrons released from the (Ra+Be) source and from the evaporation processes in the nuclei may be somewhat different.

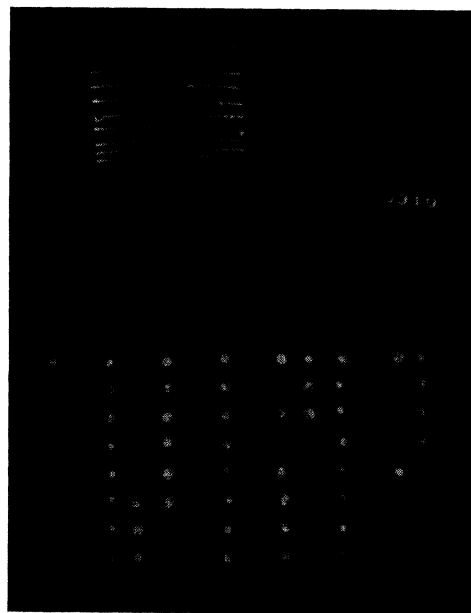
Assuming a lifetime $\tau = 155 \mu\text{sec}$. for the neutrons in our detector (see Section III), one has:

$$k = \int_5^{340} e^{-t/155} (dt/155) \approx 0.85.$$

Combining these results, we shall assume hereafter $E = 0.03$. We attribute to this figure an uncertainty of ~ 30 percent.

The absorbers used in Σ were as follows: $\Sigma = 0, \frac{1}{4}, 1-$

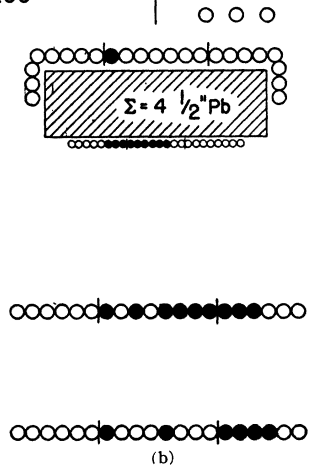
FIG. 4. Example of a picture (a) and a card (b) of a shower probably produced by an ionizing primary.



(a)

TOTAL NUMBER OF NEUTRONS: 11

UP	DOWN
2 μ sec	133 μ sec
12	158
112	284
205	300
207	
255	



(b)

TABLE I. Ratio *close/far*, for neutrons observed with various absorbers in Σ , and with a (Ra+Be) source.

Σ	<i>C/F</i>
4½-in. Pb	4.1 ±0.3
1-in. Pb	3.8 ±0.3
¼-in. Pb	3.5 ±0.5
4¾-in. Al	3.4 ±0.6
(Ra+Be) source	4.35±0.2

and 4½-in. Pb and 4¾-in. Al. The ¼- and 1-in. Pb absorbers were made of sheets $\frac{1}{16}$ in. each, evenly spaced in the 4½ in. occupied by the thickest absorber. The surface of the absorbers Σ was always 15×12 in.

The absorber *S* was either *S*=0 or *S*=6-in. Pb, with surface 21×18 in.

III. LIFETIME OF THE NEUTRONS IN THE DETECTOR

As described in Section II, the time of occurrence of each neutron pulse, assuming as time zero the instant in which the neutron that started the *MP* was recorded, could be measured with an accuracy of ±3 μsec.

The time distribution of 3100 neutron pulses is given in Fig. 5. Only pulses with delays larger than 10 μsec. have been considered, to avoid the uncertainty of the location of the pulses at the very beginning of the sweep. The curve that fits the data is drawn in Fig. 5. It indicates a lifetime $\tau = 155 \pm 5$ μsec.

The lifetime of thermal neutrons in an infinite medium of pure paraffin is about 190 μsec., due to capture by H nuclei. Taking into account the presence in our paraffin block of the B¹⁰ in the counters, the expected lifetime is ~160 μsec., close to the value experimentally found.

The value $\tau = 155$ μsec. has been used in the computation of the efficiency of our apparatus.

IV. ANGULAR DISTRIBUTION AND ENERGY OF THE NEUTRONS RECORDED

The pictures taken with the BF₃ counters in the "up-down connection" give direct information concerning the angular distribution of the neutrons produced in the nuclear events.

No significant differences have been found in the frequencies of upward and downward neutrons for any of the absorbers Σ used. This result, in agreement with preliminary results obtained in a previous experiment,⁷ indicates that the angular distribution of the moderate energy neutrons released in nuclear disintegrations is, at least in first approximation, isotropic, which supports the interpretation of these neutrons as products of nuclear evaporation.⁸

⁷ G. Cocconi and V. Cocconi Tongiorgi, Phys. Rev. **76**, 318 (1949).

⁸ For the present and the remaining discussion in this section, only experiments in which the absorber *S* was removed have been used, as the presence of *S* introduces a distortion in favor of neutrons recorded by *C* and *D*, due to backscattering and neutron production in *S* itself.

The pictures taken with the BF₃ counters in the "close-far connection" give information about the order of magnitude of the neutron energies. The ratios of pulses "close" to pulses "far," *C/F*, corrected for background and chance effects, are given in Table I for all absorbers Σ used. In the bottom row of the table is given the ratio obtained when a neutron source of 1 mC (Ra+Be) was put at the center of the space occupied by the absorbers Σ . It appears that the ratio obtained for the source is of the same order of magnitude as the ratios obtained for the neutrons recorded in our experiments.⁹ The energy spectrum of the neutrons emitted by the source ends at about 11 Mev and has a maximum¹⁰ at about 5 Mev.

A crude estimate of the neutron energies can be made as follows. Most of the pulses recorded in the "close" counters are due to neutrons slowed down to thermal energies in the neighborhood of those counters, i.e., to neutrons that crossed with moderate energies about 4 cm of paraffin. The neutrons which gave rise to pulses in the "far" counters, instead, crossed about 12 cm of paraffin. Their scattering mean free paths, are:

$$l_{\text{close}} = 1/N\sigma \approx 4 \text{ cm,}$$

$$l_{\text{far}} \approx 12 \text{ cm.}$$

With $N = 7.8 \times 10^{22}$ cm⁻³ and the cross section $\sigma = 9/E$ barns (*E* in Mev) one gets:

$$E_{\text{close}} \approx 3 \text{ Mev and } E_{\text{far}} \approx 9 \text{ Mev.}$$

V. RELATIVE NUMBER OF NEUTRAL AND CHARGED PRIMARIES OF NUCLEAR INTERACTIONS

The pictures obtained with $\Sigma = 4\frac{1}{2}$ -in. Pb and *S*=0 have been classified according to the number of counters struck in tray *a*, in order to obtain information on the relative number of neutral and charged primaries of nuclear disintegrations.

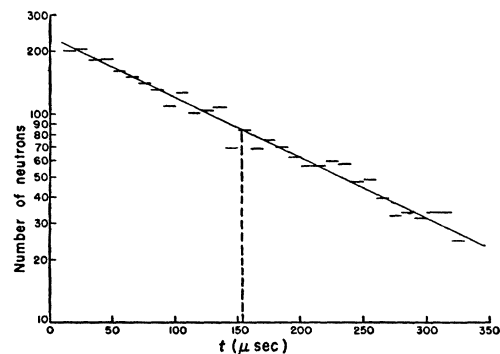


FIG. 5. Time distribution of the neutrons recorded. The lifetime of the neutrons in the detector is $\tau = 155 \pm 5$ μsec.

⁹ On the average, the energies of the neutrons emitted in nuclear evaporations seem to be slightly higher than the energies of the (Ra+Be) neutrons, although not different in order of magnitude. Therefore the use of a value for the efficiency of the apparatus based on a calibration with the (Ra+Be) source should not lead to a large error.

¹⁰ H. L. Anderson, "Neutrons from α -emitters," National Research Council, Report No. 3, Chicago (1948).

TABLE II. Rates of non-ionizing (N), single (S), and multiple (T, M) ionizing particles in counters a , and ratio R =neutral particles/charged particles evaluated for the primaries that generate the showers in Σ .

	N (hr. ⁻¹)	S (hr. ⁻¹)	T (hr. ⁻¹)	M (hr. ⁻¹)	R Lower limit	R Upper limit
$n=2$	3.95 ± 0.27	3.98 ± 0.27	1.31 ± 0.14	1.74 ± 0.17	1.0 ± 0.1	1.3 ± 0.2
$n=3, 4$	3.83 ± 0.27	4.50 ± 0.28	2.22 ± 0.22	2.61 ± 0.22	0.86 ± 0.09	1.3 ± 0.2
$n \geq 5$	1.92 ± 0.19	1.93 ± 0.20	2.72 ± 0.24	4.93 ± 0.3	1.0 ± 0.14	2.4 ± 0.3

The interpretation of the results is complicated by three phenomena: the inefficiency of tray a , the back-scattering of particles produced in the absorber Σ , and the occurrence of events accompanied by showers produced in the air or in the paraffin above the absorber Σ . The efficiency ϵ of tray a has been experimentally evaluated as close to 0.90.

If N_0, S_0, T_0, M_0 are the observed frequencies of the events in which zero, one, two, and more than two counters, respectively, have been struck in tray a , the true frequencies of the same events, N, S, T, M , are in first approximation, such that:

$$N_0 = N + S(1 - \epsilon) + T(1 - \epsilon)^2, \quad S_0 = S\epsilon + 2(1 - \epsilon)T, \\ T_0 = T\epsilon^2, \quad M_0 = M.$$

The rates (hr.⁻¹) of the events N, S, T, M are given in Table II, subdivided according to the number n of neutrons recorded, namely for $n=2, n=3$ and $4, n \geq 5$. The events in which a single neutron pulse was recorded ($n=1$) have been disregarded, as in such a category fall the chance coincidences, and practically all of the background due to spurious effects (see Section VIII). It is reasonable to assume that the number n of neutrons recorded is somewhat correlated with the energy involved in the event, hence that events with the same number n are generated by particles whose energies are of the same order of magnitude. Then, if one assumes that neutral and charged particles of the same energy have the same cross section for nuclear interactions as well as the same probability of producing particles in backward directions, the ratio $R=N/S$ for a given n , gives a lower limit of the ratio of neutral to charged particles for a given energy.

Actually, events produced by a neutral primary are

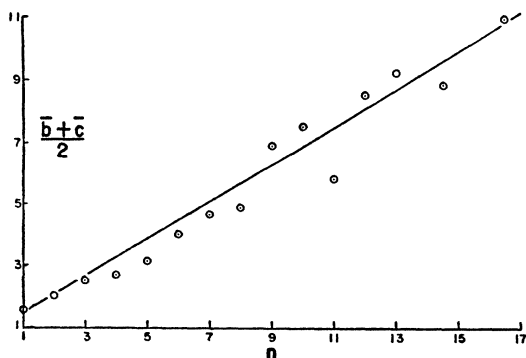


FIG. 6. Average number of counters struck per event in trays b and c (namely, $\frac{1}{2}(\bar{b} + \bar{c})$), versus number n of neutrons recorded. $\Sigma = 4\frac{1}{2}$ -in. Pb, $S=0$.

classified as being produced by ionizing particles whenever ionizing particles produced in the interaction are projected backward and whenever ionizing particles accompany the neutral primary falling on tray a .¹¹

An upper limit for the fraction of single particles scattered backward can be taken from the ratio T/S , hence an upper limit for R is approximately $N(1+T/S)/S$. The values of N/S and of $N(1+T/S)/S$ are given in Table II.

It can be seen that for all shower sizes (precisely, for all n 's) the ratio R is close to unity. This indicates that all of the events observed are produced, in first approximation, by neutral and charged particles in equal number.

It is worth remembering that the same result has been obtained for the particles which generate penetrating showers, observed both in cloud chambers and with G-M counter arrangements.¹²

VI. CORRELATION BETWEEN NUMBER OF NEUTRONS AND NUMBER OF IONIZING PARTICLES PRODUCED IN NUCLEAR INTERACTIONS

In order to obtain information about the number of neutron pulses recorded and the sizes of the ionizing events associated with them, the pictures have been classified according to the number n of the recorded neutrons. For each absorber and for each value of n , the mean numbers $\bar{a}, \bar{b}, \bar{c}$, and \bar{d} of G-M counters struck per event in trays a, b, c , and d , respectively, have been evaluated. In Fig. 6 the average of \bar{b} and \bar{c} , $\frac{1}{2}(\bar{b} + \bar{c})$, is plotted as a function of the number n of neutrons observed, for $\Sigma = 4\frac{1}{2}$ -in. Pb and $S=0$. Similar behavior has been found for the other thicknesses of Σ . It is to be noted that the numbers given on the scales of the graph are the numbers of counters struck, not the true numbers of ionizing particles and of neutrons present. If n neutrons are recorded, the most probable number of neutrons present is approximately proportional to n . However, a G-M counter that records one ionizing particle is insensitive to further particles striking at the same time. Therefore, the most probable number of ionizing particles increases more rapidly than does the number of counters struck, this effect becoming strong when the probability is great for more than one particle to fall on a single counter. Consequently, if we were

¹¹ The pictures which could be recognized as arising from events accompanied by a shower (on the basis of counters s being struck and of the general appearance of the picture) have been disregarded. However, small showers can hardly be recognized as such.

¹² W. D. Walker, Phys. Rev. 77, 686 (1950).

TABLE III. Ratios of average numbers of counters struck in trays c and d , with and without the absorber $S=6$ -in. Pb.

		$n=3$	$n=4$	$n \geq 5$
$\Sigma=4\frac{1}{2}$ -in. Pb, $S=0$	$\frac{\bar{c}}{\bar{d}} = \frac{\omega_c}{\omega_d}$	1.8	1.9	1.6
$\Sigma=4\frac{1}{2}$ -in. Pb, $S=6$ -in. Pb	\bar{c}/\bar{d}	4.9	4.2	4.3
	$\frac{\bar{c}}{\bar{d}} \cdot \frac{\omega_d}{\omega_c}$	2.7	2.2	2.7

TABLE IV. Frequency (hr.⁻¹) of events, versus number n of neutrons recorded, for $S=0$ and different absorbers in Σ .

n	$\Sigma=0$, $S=0$	$\Sigma=4\frac{1}{2}$ -in. Pb, $S=0$	$\Sigma=1$ -in. Pb, $S=0$	$\Sigma=\frac{1}{4}$ -in. Pb, $S=0$	$\Sigma=4\frac{1}{2}$ -in. Al, $S=0$
1	7.1±0.3	7.4 ±0.5	7.4 ±0.4	2.7 ±0.3	2.7 ±0.3
2	0.4±0.06	10.2 ±0.4	5.1 ±0.3	1.5 ±0.1	0.85±0.07
3	0.04	7.7 ±0.4	2.7 ±0.2	0.47±0.5	0.07±0.02
4		5.0 ±0.3	1.1 ±0.1	0.09±0.02	0.05
5		3.7 ±0.3	0.22 ±0.06	0.05±0.02	
6		2.5 ±0.2	0.13 ±0.04		
7		1.5 ±0.2	0.044±0.025		
8		1.1 ±0.2	0.015		
9		0.69±0.11			
10		0.58±0.10			
11		0.44±0.09			
12-13		0.19±0.08			
14-15		0.06±0.04			
≥16		0.025			

able to plot the actual number of ionizing particles versus the actual number of neutrons, the graph in Fig. 6 would have a much greater slope at large values of $\frac{1}{2}(\bar{b} + \bar{c})$, and a not much greater slope at small values.

This indicates that the number of ionizing particles probably increases more rapidly with increasing shower size (or primary energy) than does the number of moderate energy neutrons.

In Fig. 7 are given examples of the distribution of the number of G-M counters struck in tray b , for a given number of neutrons observed, namely for $n=2$, $n=4$, $n=6$ ($\Sigma=4\frac{1}{2}$ -in. Pb, $S=0$). The curves do not show a maximum, but exponential-like distributions, being the steeper the lower the value of n . Here again, if one could plot on the abscissae the average number of particles in trays b and c , instead of the average number of counters struck, it would strongly stretch the lengths of the tails of the curves. The results seem quite interesting as they show that a large number of neutrons of moderate energy can be released in events in which very few ionizing particles are present, and that, vice versa, a large number of ionizing particles does not necessarily imply the presence of a large number of neutrons.

VII. PENETRATING POWER OF THE IONIZING PARTICLES PRODUCED IN NUCLEAR INTERACTIONS

The average numbers, \bar{c} and \bar{d} , of counters struck per event in trays c and d have been computed, as a function of the number n of neutrons recorded, for the following arrangements of absorbers: $\Sigma=0$, $S=0$; $\Sigma=4\frac{1}{2}$ -in. Pb, $S=0$; $\Sigma=0$, $S=6$ -in. Pb; $\Sigma=4\frac{1}{2}$ -in. Pb, $S=6$ -in. Pb.

The figures obtained for $\Sigma=0$, $S=0$, and $\Sigma=0$, $S=6$ -in. Pb have been used to correct the results obtained for $\Sigma=4\frac{1}{2}$ -in. Pb, $S=0$, and $\Sigma=4\frac{1}{2}$ -in. Pb, $S=6$ -in. Pb, respectively. When no absorber was present in $S(S=0)$ this background was smaller than five percent of the events recorded, for all events with $n \geq 2$. When the absorbers S was present ($S=6$ -in. Pb), the background was smaller than 10 percent of the events recorded, for all events with $n \geq 3$. Therefore, for all events with $n \geq 3$, the uncertainties involved in the background correction applied are probably immaterial.

The ratios \bar{c}/\bar{d} obtained for $\Sigma=4\frac{1}{2}$ -in. Pb, $S=0$, and $\Sigma=4\frac{1}{2}$ -in. Pb, $S=6$ -in. Pb, corrected as indicated above, are given in Table III.

Assuming that the ratio \bar{c}/\bar{d} obtained with $S=0$ equals the ratio ω_c/ω_d of the solid angles subtended at Σ by trays c and d , respectively, one gets the values given in the last row of Table III, which give the effect due to the presence of S . It appears that approximately 40 percent of the particles emerging from $4\frac{1}{2}$ -in. Pb are capable of crossing 6-in. Pb, and that the average penetration of the particles is the same for events in which different numbers of neutrons have been recorded.

To check this result, an attempt has been made to select from among all the pictures taken with $\Sigma=4\frac{1}{2}$ -in. Pb, $S=0$ and $\Sigma=4\frac{1}{2}$ -in. Pb, $S=6$ -in. Pb only those showing events that could be recognized as originating in Σ . In this case no background correction was needed. The ratios c/d obtained in this way were found to be in agreement with the figures given in Table III.

VIII. FREQUENCY OF NUCLEAR DISINTEGRATIONS AS A FUNCTION OF THE NUMBER OF NEUTRONS RECORDED

The frequencies $f(n)$ per hour of the events recorded with $S=0$ and $\Sigma=0$, $\frac{1}{4}$ -, 1-, $4\frac{1}{2}$ -in. Pb and $4\frac{1}{2}$ -in. Al

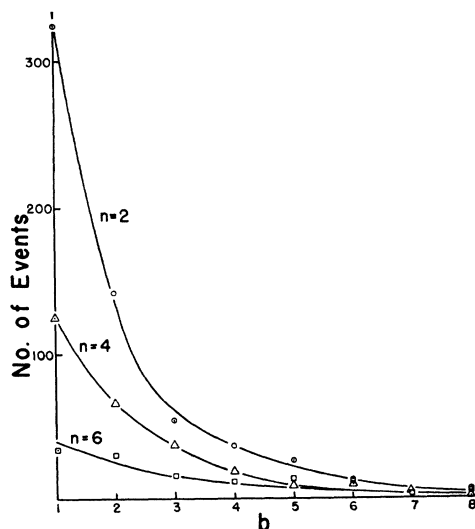


FIG. 7. Distribution of the number of counters struck per event in tray b for $n=2$, $n=4$, and $n=6$. $\Sigma=4\frac{1}{2}$ -in. Pb, $S=0$.

have been determined, as a function of the number, n , of neutrons of moderate energy recorded.

The results are given in Table IV with their standard errors. All the figures referring to absorbers $\Sigma \neq 0$ have been corrected for the background effects recorded with $\Sigma = 0$.

The data for $\Sigma \neq 0$ are also plotted in Fig. 8. The curves given in the figure are not drawn according to the experimental points; they are the results of the calculations described in Section IX. Inspection of Table IV and of Fig. 8 leads one to the following qualitative deductions.

(a) With $\Sigma = 0$ no events have been recorded which show a high number of neutrons of moderate energy. Actually in 94 percent of these events only *one* neutron was recorded (i.e., the neutron *required* by the apparatus to create a *MP*). The reason for this is that about one-half (4 hr.^{-1}) of the events recorded with $\Sigma = 0$ are due to chance coincidences between a single neutron and a single ionizing particle capable of giving a coincidence (*b, c*). The remaining events are mostly due to nuclear disintegrations produced in the paraffin; in such events neutrons are produced with a rather low multiplicity, and furthermore the geometrical efficiency of our apparatus for detecting them is appreciably lower than it is for detection of neutrons produced in the absorbers Σ . This result is remarkably important for our experiment since, as a consequence, the background correction applied to the data taken with $\Sigma \neq 0$ is immaterial for all the events in which two or more than two neutrons ($n \geq 2$) have been recorded.¹³

(b) Higher neutron multiplicities have been recorded, on the average, in association with nuclear disintegrations taking place in Pb than in Al.

(c) The neutron multiplicities recorded in association with nuclear disintegrations occurring in lead are higher (on the average) the thicker the absorber.

(d) The frequencies of the events recorded with a given absorber decrease strongly with increasing n .

(e) The rate of decrease is different for different thicknesses of a given material, and for the different materials. It can be described by the following expressions:

$$\begin{aligned} \text{for } \Sigma = 4\frac{1}{2}\text{-in. Pb, } & f(n) \sim e^{-0.46n}, \\ \text{for } \Sigma = 1\text{-in. Pb, } & f(n) \sim e^{-1.0n}, \\ \text{for } \Sigma = \frac{1}{4}\text{-in. Pb, } & f(n) \sim e^{-1.36n}, \\ \text{for } \Sigma = 4\frac{3}{4}\text{-in. Al, } & f(n) \sim e^{-1.8n}. \end{aligned}$$

Let us consider the data obtained with lead absorbers. The fact that the slope of the curves $f(n)$ is lower the thicker the absorber Σ can be explained with one of the following assumptions.

(1) The nuclear disintegrations occurring in the thicker absorbers, on the average, involve energies higher than those involved in events taking place in thin absorbers, and high energy events produce *in a single act* a much greater number of neutrons than do lower energy events.

(2) Each nuclear disintegration releases, on the average, a number of neutrons of moderate energy practically independent of the energy involved in the process, but there is a finite probability of release also of particles capable of giving rise to further reactions in which more neutrons are produced, the probability of such secondary reactions being larger in the thicker absorbers.

¹³ The results given in Table IV and plotted in Fig. 8 for $n = 1$ are somewhat uncertain as the correction for the background is certainly approximate. In fact, the presence of the absorber modifies slightly the rates of chance coincidences and affects to some extent the events occurring in the paraffin. No specific use of these data is made in the following discussion.

(3) A mixture of the two preceding assumptions is true; i.e., cascade-like processes take place in the absorbers, and furthermore, energetic processes release in each act more neutrons, on the average, than do low energy events.

If assumption (1) is correct, the frequencies of the events showing a given number of neutrons, recorded for absorbers of various thicknesses, cannot increase, with increasing thickness of the absorber, more than in proportion to the absorber thickness. Furthermore, the slopes of the curves obtained for large values of n (for which all events presumably have a probability close to unity of being recorded, for all thicknesses of the absorber) must be equal.

Neither of these conditions is fulfilled by our experimental points. The ratio of the frequencies recorded with $\Sigma = 4\frac{1}{2}$ -in. Pb and with $\Sigma = \frac{1}{4}$ -in. Pb (ratio of thickness = 18) is larger than 18 for all $n \geq 3$. For $n = 6$ this ratio is already close to 200. Furthermore, up to 17 neutron pulses have been observed on our sweep, with $\Sigma = 4\frac{1}{2}$ -in. Pb. This corresponds to an actual number of neutrons produced in Σ of the order of $17/E \cong 500$ ($E = 0.03$ is the efficiency of the apparatus). Such a huge number of neutrons is certainly not conceivable as the product of only one or even a few evaporations of Pb nuclei.

This indicates that assumption (1) is not consistent with the experimental results, and therefore either assumption (2) or (3) is true. Our data do not supply arguments for discrimination between these two possible cases.

Anyway, we can conclude that the existence of a cascade-like process of nuclear interactions is clearly proved by our data. The neutrons we record are produced both in the primary and in the secondary acts of the process, the contribution of the secondary acts being the more important the thicker the absorber used.

More precise conclusions will be obtained from the

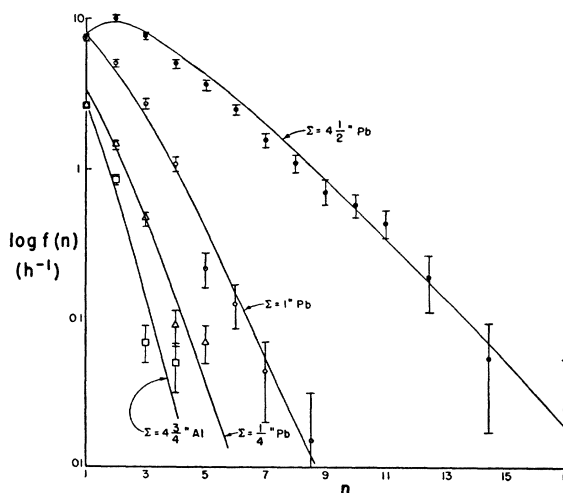


FIG. 8. Frequency (hr.^{-1}) of the events in which n neutrons were recorded versus n , for $\Sigma = 0$ and $\Sigma = \frac{1}{4}$ -in. Pb, 1-in. Pb, $4\frac{1}{2}$ -in. Pb, $4\frac{3}{4}$ -in. Al. The curves are the result of the analysis of Section IX.

quantitative treatment of the problem given in the following section.

IX. MULTIPLICITY SPECTRA OF THE MODERATE ENERGY NEUTRONS RELEASED IN NUCLEAR INTERACTIONS

The functions $f(n)$ obtained in Section VIII from the experimental data represent the frequencies of the events occurring in Σ , in which n neutrons were recorded by our apparatus.

It is our purpose here to evaluate, from the functions $f(n)$, the functions $I(\nu)$, which give the frequencies of the events leading to the production of ν neutrons of moderate energies. We wish it to be clear that ν is the *true number* of moderate energy neutrons produced in the events, while $n \leq \nu$ is the number of neutrons recorded by our apparatus; $I(\nu)$ is the *true frequency* of the events with ν neutrons, while $f(n)$ is the frequency recorded by our apparatus for the events with n recorded neutrons. We shall call the functions $I(\nu)$, the "*multiplicity spectra*" of the moderate energy neutrons produced in nuclear disintegrations occurring in the absorbers Σ used.

It is quite plain that the functions $f(n)$ do not reproduce the functions $I(\nu)$, as the events occurring in Σ are weighted by our apparatus according to their probability of being detected; i.e., according to their probability of giving a master pulse.

As all of the events with $\nu \geq n$ have a finite probability of having n neutrons recorded, one must write

$$f(n) = \sum_{\nu=n}^{\infty} I(\nu) \cdot G(\nu, n) \cdot \Pi(n) \cdot P_{b,c}(\nu).$$

$G(\nu, n)$ is the probability that, out of ν -neutrons produced in an event, n are recorded in the time interval between 5 and 340 $\mu\text{sec.}$, and is given by¹⁴

$$G(\nu, n) = \binom{\nu}{n} E^n (1-E)^{\nu-n},$$

where E , the over-all efficiency of our system for recording each neutron, is 0.03, as explained in Section II.

$\Pi(n)$ is the probability that at least one of the n neutrons recorded falls within the time interval from 5 to 15 $\mu\text{sec.}$ to trigger the sweep. One has:

$$\Pi(n) = 1 - \left(\int_{15}^{340} (dt/\tau) e^{-t/\tau} / \int_5^{340} (dt/\tau) e^{-t/\tau} \right)^n = 1 - r^n.$$

With $\tau = 155 \mu\text{sec.}$, $r = 0.93$.

The probability $P_{b,c}(\nu)$ of getting a particle capable of producing a coincidence (b, c) cannot, unfortunately, be computed correctly. However (as shown by the

¹⁴ In all of our previous papers on neutrons of moderate energy, an incorrect expression was used for the calculation of the probability of recording n neutrons, since we replaced $\exp(-En)$ by $(1-E)^n$. The two expressions differ only in the terms of order higher than the second, so that the numerical results remain unchanged.

curve in Fig. 6), the average numbers of particles recorded in trays b and c steadily increase when the number of neutrons recorded increases. For the sake of simplicity then we shall put

$$P_{b,c}(\nu) = 1.$$

This assumption is probably near the truth for the events in which large number of neutrons are recorded, while it certainly is incorrect for small values of n . This approximation will not allow us to utilize the absolute values of the multiplicity spectra we shall obtain from this calculation. However, we feel that the main characteristics of the processes will not be strongly affected by it.

We can write finally:

$$f(n) = \sum_{\nu=n}^{\infty} I(\nu) \cdot \binom{\nu}{n} E^n \cdot (1-E)^{\nu-n} \cdot (1-r^n). \quad (1)$$

Equation (1) is to be satisfied by the introduction of an appropriate function for $I(\nu)$. The following working hypotheses have been tried: (a) All events have the same neutron multiplicity (in which case the sum in Eq. (1) is reduced to a single term); (b) $I(\nu)$ is a power spectrum: $I(\nu) \sim \nu^{-\gamma}$; (c) $I(\nu)$ is an exponential spectrum: $I(\nu) \sim e^{-a\nu}$. It has been found that assumptions (a) and (b) cannot satisfy the experimental data. Assumption (c), instead, can be worked out successfully. In this case, the solution of Eq. (1) is

$$f(n) = K(1-r^n) \cdot (E \cdot e^{-a})^n / [1 - (1-E) \cdot e^{-a}]^{n+1}.$$

The functions $I(\nu)$ which satisfy the experimental points are as follows:

$$\begin{aligned} \text{for } \Sigma = 4\frac{1}{2}\text{-in. Pb, } & I(\nu) = 10e^{-0.02\nu} \text{ per hour,} \\ \text{for } \Sigma = 1\text{-in. Pb, } & I(\nu) = 30e^{-0.06\nu}, \\ \text{for } \Sigma = \frac{1}{4}\text{-in. Pb, } & I(\nu) = 30e^{-0.1\nu}, \\ \text{for } \Sigma = 4\frac{3}{4}\text{-in. Al, } & I(\nu) = 50e^{-0.17\nu}. \end{aligned} \quad (2)$$

The functions given above are the differential multiplicity spectra of the moderate energy neutrons produced in the various absorbers Σ .

The functions $f(n)$ obtained by substitution of these spectra in Eq. (1) are the curves drawn in Fig. 8.

X. AVERAGE NEUTRON MULTIPLICITIES

From the multiplicity spectra (2) given in the preceding section, one derives that the average multiplicities $\bar{\nu} = 1/a$ of the moderate energy neutrons released by the nuclear disintegrations occurring in the absorbers used, are as follows:

$$\begin{aligned} \text{for } \Sigma = 4\frac{1}{2}\text{-in. Pb, } & \bar{\nu} = 50, \\ \text{for } \Sigma = 1\text{-in. Pb, } & \bar{\nu} = 17, \\ \text{for } \Sigma = \frac{1}{4}\text{-in. Pb, } & \bar{\nu} = 10, \\ \text{for } \Sigma = 4\frac{3}{4}\text{-in. Al, } & \bar{\nu} = 6. \end{aligned}$$

The absolute values of the coefficients a in the exponents of the spectra, hence the $\bar{\nu}$'s, can be in error by a factor as large as 2, mainly because of the uncertainty in the

estimate of efficiency E of the apparatus and of the extrapolation of the multiplicity spectra to low values of n . However, the relative values of $\bar{\nu}$ are believed to be correct within 20 percent.

The large increase with the thickness of the absorber of the average number of neutrons emerging from it confirms the strong secondary neutron production, as deduced in the qualitative discussion of the data.

Analogous variation of $\bar{\nu}$ with the thickness of the absorber was obtained in the preliminary experiment previously quoted.⁷ There, however, the lack of information about the multiplicity spectra of the neutrons for the various absorbers left open the problem of whether the large number of neutrons emerging from thick absorbers were produced in a single act or in several successive acts.

In the light of the present experiment it clearly appears that when one concerns himself with the problem of the multiplicity of neutrons released in a given material, the most interesting and meaningful figure is the average number of neutrons released, in the material considered, *by a single nuclear interaction*. This figure can be derived experimentally only if the thickness of the absorber in which the processes take place is small enough to make the probability of secondary interactions practically negligible.

As a rule, we think that a reasonably good value for the multiplicity of neutron production in a single interaction can be obtained if the thickness of the absorber is smaller than, say, one-tenth to one-twentieth of the interaction mean free path (in the given material) of the radiation causing nuclear disintegrations (N -component). If one assumes mean free paths corresponding to the geometrical nuclear cross sections, the "thin target condition" stated above is fulfilled, in lead, if the thickness of the absorber is smaller than about 10 g/cm².

The figure $\bar{\nu}=10$ obtained with $\Sigma=\frac{1}{4}$ -in. Pb (7 g/cm²), therefore, must be considered as our best approximation to the average multiplicity of the moderate energy neutrons released in Pb, in a single nuclear disintegration induced by the N -component. The value obtained for $\Sigma=1$ -in. Pb (28 g/cm²) shows that secondary interactions already play a considerable role in that absorber.

For aluminum, the "thin target condition" is fulfilled only if the absorber is smaller than about 7 g/cm². The thickness of the Al absorber we used was about five times this value. The result we obtained with $\Sigma=4\frac{3}{4}$ -in. Al, $\bar{\nu}=6$, indicates that the average multiplicity of a single nuclear interaction in Al is smaller than that, probably close to 2 or 3.

If the "thin target condition" is not satisfied, the average number of neutrons measured depends not only on the material used, but also on its thickness. This point is particularly important when comparisons of multiplicities of neutron production in different materials are made.

Of course, the thin target condition is the less important the lower the energies involved in the processes investigated. Nuclear events in which no relativistic particles are emitted, probably cannot induce many secondary interactions, and the multiplicities of the neutrons produced in these events are expected to be close to the multiplicities of neutrons released in a single act.

On this line of reasoning we now interpret the fact that the average multiplicity measured for neutrons released in nuclear disintegrations occurring in 2-in. Pb was found to be from 30 to 60 when association with a penetrating shower^{2,7} or an extensive shower⁴ was required; it was found to be only about 9 when such requirements were not made, since in the latter case neutrons mostly released in low energy stars were recorded.¹⁵

XI. COMPARISON OF MULTIPLICITY SPECTRA OF MODERATE ENERGY NEUTRONS AND OF HEAVILY IONIZING PRONGS OF STARS OBSERVED IN PHOTOGRAPHIC PLATES

It is interesting to compare the multiplicity spectra obtained for neutrons of moderate energy produced in nuclear disintegrations with the multiplicity spectra obtained for the stars of heavily ionizing particles observed in photographic plates.

The frequency $F(p)$ of stars with p heavily ionizing prongs, is given by

$$F(p) \cong e^{-\alpha p}$$

with $\alpha=0.3$ to 0.5 .¹⁶

The neutron spectra given by Eqs. (2) also have an exponential form.

On the basis of the discussion given in Section X, we can assume that the neutrons produced in $\Sigma=\frac{1}{4}$ -in. Pb collect only a very small contribution from secondary nuclear processes, hence we can compare the exponent $a=0.1$ with the values obtained for α . The fact that a is somewhat smaller than the figures obtained for α can be accounted for easily by the facts that no Coulomb barrier hinders the escape of neutrons from nuclei, that the average energy involved in the processes we observed is probably higher than that involved in the evaporations observed in photographic plates, and that the evaporations observed in the plates occur mostly in Ag and Br nuclei whose atomic numbers are lower than that of Pb.

Although the measurements are statistically quite poor, the results obtained with $\Sigma=4\frac{3}{4}$ -in. Al give $a=0.17$, and this value must probably be increased by a factor of 2 or so to correct for secondary interactions. This can be taken as an indication that, as expected, the exponent a increases when the atomic number decreases.

¹⁵ V. Cocconi Tongiorgi, Phys. Rev. 76, 517 (1949).

¹⁶ See, for example, B. Rossi, M.I.T. Report No. 26 (1944), and M. Addario and S. Tamburino, Phys. Rev. 76, 983 (1949).

XII. TENTATIVE ANALYSIS OF THE CASCADE PROCESS FOR NUCLEAR INTERACTIONS

A discussion of the features of the cascade process for nuclear interactions requires the use of parameters which are up to now unknown: the mean free path of the N -component as a function of energy, the angular distribution, the energy and multiplicity spectra of secondary particles emitted, etc.

The information we can derive from our experiments is that the multiplicity spectrum of the neutrons of moderate energies emitted in nuclear disintegrations is $\sim \exp(-0.1\nu)$ when the phenomena occur in a Pb layer of $\frac{1}{4}$ -in., where secondary processes have little probability of taking place, whereas the phenomena occurring in $4\frac{1}{2}$ -in Pb, where the contribution of secondary processes is important, produce neutrons with a multiplicity spectrum proportional to $\exp(-0.02\nu)$.

Several models can be worked out to account for such a behavior. Although the results of the calculations depend strongly on the assumptions arbitrarily introduced, we thought it worth while to show how the experimental results can be described with some simple assumptions.

To describe the phenomena occurring in the absorber $\Sigma = 4\frac{1}{2}$ -in. Pb the following model is assumed. A particle belonging to the N -component, falling on the Pb absorber Σ , produces nuclear disintegrations with a mean free path $\lambda = 1/N\sigma$ where σ is the geometrical cross section of the Pb nuclei ($\lambda = 160$ g/cm²).

A primary nuclear disintegration produces: (a) ν_1 -neutrons of moderate energy, isotropically distributed, not capable of inducing further nuclear disintegrations. The probability of ν_1 such neutrons being produced is given by $H(\nu_1) = (1 - e^{-a}) \exp(-a\nu_1)$. On the basis of the experimental results obtained with $\Sigma = \frac{1}{4}$ -in. Pb, we put $a = 0.1$. (b) N_1 particles (fast neutrons, fast protons, π -mesons) emitted in the forward direction, capable of producing further disintegrations with the same mean free path λ as that of the primary radiation. In each of the secondary reactions induced by these particles, neutrons of moderate energies are produced, with the same angular distribution and the same probability as specified in (a).

The probability that N_1 of these fast particles are produced is assumed to be expressed by an exponential function, $F(N_1) = (1 - e^{-b}) \exp(-bN_1)$. The coefficient b is the unknown of the problem. Of course, $1/b = N_1$ will be the average number of such particles. For the sake of simplicity, the assumption is introduced that the energy degradation in the primary act and/or the energy of the primary particle are such as to make the importance of tertiary processes negligible in the absorber Σ considered (the thickness of Σ is $h = 128$ g/cm² = $\frac{4}{5}$ of a mean free path). For simplicity we consider here the vertical direction only.

The probability $P(\nu)$ of having ν -neutrons emerging from Σ can be written as the product of the probabilities of ν_1 -neutrons being produced in the primary act,

and of $\nu_2 = (\nu - \nu_1)$ neutrons being produced in secondary reactions. Hence

$$P(\nu) = \sum_{\nu_1=0}^{\nu} H(\nu_1) \cdot J(\nu - \nu_1). \quad (3)$$

$J(\nu - \nu_1)$ is given by:

$$J(\nu - \nu_1) = \sum_{s=1}^{\infty} g(s) \cdot \Pi(s, \nu - \nu_1)$$

where $g(s)$ is the probability that s secondary disintegrations happen in the absorber, and $\Pi(s, \nu - \nu_1)$ is the probability that the s secondary disintegrations give rise to $(\nu - \nu_1)$ neutrons in total.

If h is the thickness of the absorber,

$$g(s) = \frac{1}{\lambda} \int_0^h \frac{e^{-x/\lambda}}{1 - e^{-h/\lambda}} \cdot \sum_{N_1=0}^{\infty} F(N_1) \cdot \binom{N_1}{s} \times [1 - \exp(-(h-x)/\lambda)]^s [\exp(-(h-x)/\lambda)]^{N_1-s} dx$$

and

$$\Pi(s, \nu - \nu_1) = \frac{(s + \nu - \nu_1 - 1)!}{(s - 1)! (\nu - \nu_1)!} (1 - e^{-a})^s \exp[-a(\nu - \nu_1)].$$

After performing the sums and the integral in expression (3), one finds¹⁷ that the probability $P(\nu)$ that ν -neutrons emerge from the absorber $\Sigma = 4\frac{1}{2}$ -in. Pb is given by:

$$P(\nu) = \frac{1 - e^{-a}}{\lambda} \frac{e^{-a\nu}}{1 - m} (1 - \beta) \left\{ \lambda m B^{-(\nu+1)} \cdot C \times \left\{ \frac{\exp[-\nu(\beta - D)U_1]}{U_1} \frac{\exp[-\nu(\beta - D)U_2]}{U_2} + [D - \nu(\beta - D)] [E_i(-Y_2) - E_i(-Y_1)] \right\} - \{ \lambda + m[\beta h - \lambda + \beta \lambda \ln(1 - \beta m)/(1 - \beta)] \} \right\} \quad (4)$$

with:

$$\begin{aligned} \beta &= e^{-b}, & m &= e^{-h/\lambda}, & B &= 1 - \beta(1 - e^{-a}), \\ C &= \exp\{-\nu/2(D - \beta)^2[(U_1 + U_2)/2]^2\}, \\ D &= \beta e^{-a}/[1 - \beta(1 - e^{-a})], \\ U_1 &= m/(1 - mD), & U_2 &= 1/(1 - D), \\ Y_1 &= U_1(\beta - D)\nu, & Y_2 &= U_2\nu(\beta - D). \end{aligned}$$

Equation (4) has been solved for various values of $b = -\ln\beta$ and it has been found that the function $P(\nu)$ is very close to an exponential, $\sim \exp(-a'\nu)$, as required to satisfy the experimental result. It fits the data, i.e., it gives $a' \approx 0.02$, for $b = 0.1$. This would indicate that the fast particles released in nuclear disintegrations capable of inducing further nuclear processes, have a multiplicity spectrum analogous to that found for

¹⁷ We are grateful to Professor R. P. Feynman for assistance in the solution of this equation.

moderate energy neutrons. In other words, with the assumptions introduced in our model, an average number $\bar{N}_1 \approx 10$ of fast particles are required to describe our experimental results.

The same model of the nuclear cascade process can be worked out more easily and can be extended to include tertiary, quaternary, etc. interactions, if one limits oneself to the consideration of the average numbers of particles emitted, rather than to their multiplicity spectra.

Let Π_0 be the number of primary particles falling on the absorber Σ , and Π, S, T, \dots the numbers of primary, secondary, tertiary, etc. fast particles at the depth x in the absorber. Let $\bar{N}_1, \bar{N}_2, \bar{N}_3, \dots$ and $\bar{\nu}_1, \bar{\nu}_2, \bar{\nu}_3, \dots$, respectively, be the average number of fast particles and of moderate energy neutrons produced in primary, secondary, tertiary, etc. acts.

One has:

$$\Pi = \Pi_0 \cdot e^{-x/\lambda}. \tag{5a}$$

For secondary particles, the following diffusion equation can be written:

$$dS/dx = (\bar{N}_1 \Pi - S)/\lambda,$$

which gives

$$S = \bar{N}_1 \Pi_0 \cdot x e^{-x/\lambda}. \tag{5b}$$

Analogous differential equations can be written for the tertiary, quaternary, etc. particles and the solutions are:

$$T = \bar{N}_1 \bar{N}_2 \Pi_0 \cdot \frac{1}{2}! (x/\lambda)^2 e^{-x/\lambda} \tag{5c}$$

$$Q = \bar{N}_1 \bar{N}_2 \bar{N}_3 \Pi_0 \cdot \frac{1}{3}! (x/\lambda)^3 e^{-x/\lambda}. \tag{5d}$$

The total number $\bar{\nu}$ of moderate energy neutrons produced in the thickness h of the absorber Σ is then:

$$\bar{\nu} = \int_0^h \left(\frac{\Pi}{\lambda} + \frac{S}{\lambda} + \frac{T}{\lambda} + \dots \right) dx$$

where Π, S, T, \dots are given by the expressions (5). For comparison with the experiment, we consider

$$\bar{\nu}_h = \bar{\nu} / \Pi_0 (1 - e^{-h/\lambda});$$

i.e., the average number of neutrons generated in a nuclear cascade process by a primary particle *interacting in the absorber* Σ . One has:

$$\begin{aligned} \bar{\nu}_h = & \bar{\nu}_1 + \bar{\nu}_2 \bar{N}_1 \left(1 - \frac{h}{\lambda} \frac{e^{-h/\lambda}}{1 - e^{-h/\lambda}} \right) \\ & + \bar{\nu}_3 \bar{N}_1 \bar{N}_2 \left[1 - \frac{h}{\lambda} \frac{e^{-h/\lambda}}{(1 - e^{-h/\lambda})} \left(1 + \frac{1}{2!} \frac{h}{\lambda} \right) \right] \\ & + \bar{\nu}_4 \bar{N}_1 \bar{N}_2 \bar{N}_3 \left[1 - \frac{h}{\lambda} \frac{e^{-h/\lambda}}{(1 - e^{-h/\lambda})} \right. \\ & \quad \left. \times \left(1 + \frac{1}{2!} \frac{h}{\lambda} + \frac{1}{3!} \left(\frac{h}{\lambda} \right)^2 \right) \right] + \dots \end{aligned}$$

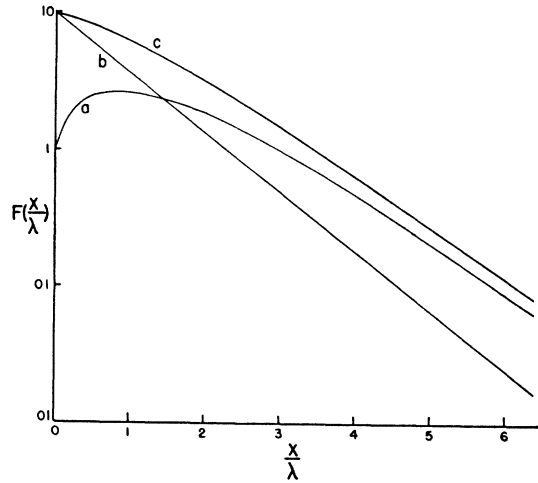


FIG. 9. Analysis of the absorption curve in lead of the radiation producing the nuclear disintegrations observed in non-electron sensitive photographic plates. Curve a: absorption of the radiation producing high energy events. Curve b: absorption of the radiation producing low energy events. Curve c: sum of curves a and b.

With $\lambda = 160 \text{ g/cm}^2$ and $h = 128 \text{ g/cm}^2$, one gets:

$$\bar{\nu}_h = \bar{\nu}_1 + 0.65 \bar{\nu}_2 \bar{N}_1 + 0.51 \bar{\nu}_3 \bar{N}_1 \bar{N}_2 + 0.47 \bar{\nu}_4 \bar{N}_1 \bar{N}_2 \bar{N}_3 + \dots \tag{6}$$

If we introduce the same assumptions as those used in the first treatment of the problem, namely,

$$\begin{aligned} \bar{\nu}_1 = \bar{\nu}_2 = 10 \\ \bar{N}_2 = \bar{N}_3 = \dots = 0, \end{aligned}$$

we deduce that in order to have $\bar{\nu}_h = 50$ as experimentally found, we must have $\bar{N}_1 = 6.2$.

The comparison of this figure with the result of the previous calculation, $\bar{N}_1 = 10$, gives an idea of the error introduced by considering the average numbers of particles rather than their multiplicity spectra.

It is worth noticing that with $h = 7 \text{ g/cm}^2$ ($\Sigma = \frac{1}{4}$ -in. Pb), introducing $\bar{N}_1 = 6.2$, one gets $\bar{\nu}_h = 11$, which is close enough to 10 to justify our statement that such an absorber is a "thin target;" i.e., makes the probability of secondary disintegrations practically negligible.

For $h = 28 \text{ g/cm}^2$ ($\Sigma = 1$ -in. Pb) one gets $\bar{\nu}_h = 16$, in good agreement with the experimental figure $\bar{\nu} = 17$.

If the cascade is not stopped at the second generation, and it develops down to tertiary, quaternary, etc. acts, it clearly appears from formula (6) that a smaller multiplicity of fast particles is required in each act.

In our opinion, however, only a small fraction of the nuclear cascades should be able to propagate that far, as most of the primary particles of the N -component have energies not very far above the minimum required to initiate the cascade process.

Nevertheless, the few particles of enough energy to allow tertiary, etc. processes to be probable, likely account for the few showers with very high neutron multiplicity.

Certainly a treatment which is to be valid both for

very large and for small values of the neutron multiplicity must allow the number of generations to be variable with the primary energy, even if the mean free path and the multiplicity in each act are not necessarily variable. In other words, the energy dependence and energy spectra cannot be ignored in a precise treatment.

XIII. AN INTERPRETATION OF THE EXPERIMENTAL RESULTS FOR THE ABSORPTION MEAN FREE PATH OF THE N -COMPONENT PRODUCING NUCLEAR DISINTEGRATIONS IN PHOTOGRAPHIC PLATES

From the analysis of the nuclear events given above it turns out that the particles of the N -component giving rise to moderate energy neutrons can be subdivided in two categories: (a) Particles of high energies capable of producing stars with relativistic particles, hence capable of inducing further nuclear disintegrations. Their total number under a thickness x of an absorber is (as shown in Section XII, Eqs. (5)):

$$\Pi + S + T + \dots + \Pi_0 e^{-x/\lambda} \times \left[1 + \bar{N}_1 \frac{x}{\lambda} + \bar{N}_1 \bar{N}_2 \cdot \frac{1}{2!} \left(\frac{x}{\lambda} \right)^2 + \dots \right].$$

With the same assumptions as in Section XII, namely, $\bar{N}_1 = 6.2$, $\bar{N}_2 = \bar{N}_3 = \dots = 0$, and $\lambda = \text{constant}$, these particles are absorbed proportionally to $e^{-x/\lambda} [1 + 6(x/\lambda)]$ (curve a in Fig. 9). (b) Particles of not very high energies, capable of producing only stars without relativistic particles. These particles are absorbed in a thickness x of a given material with exponential law, i.e., proportionally to $e^{-x/\lambda}$ (curve b in Fig. 9), where λ is the interaction mean free path of such a radiation in the material considered.

Let us now consider the nuclear disintegrations produced in non-electron sensitive photographic plates, by the N -component. When an absorption curve of the radiation producing such disintegrations is made, one has to expect that the intensity of this radiation under a thickness x of material is described by an expression like the following, which is the sum of the two components (a) and (b):

$$F(x/\lambda) = B e^{-x/\lambda} + A e^{-x/\lambda} [1 + 6(x/\lambda)],$$

where A and B are the intensities of the two components (a) and (b) falling on the absorber.

Curves a and b in Fig. 9 are plotted with the assumption¹⁸ that $B/A = 10$. Curve c represents the sum of curves a and b, hence the function $F(x/\lambda)$. It can be seen that for small values of x , $F(x/\lambda)$ approaches an exponential curve with an absorption mean free path $\lambda_{obs} \approx 2\lambda$.

The experimental results of several authors¹⁹ agree in indicating that the absorption mean free path λ_{obs} in Pb of the radiation producing nuclear disintegrations, is close to 300 g/cm². On the basis of the interpretation given above, such a figure is consistent with the interaction mean free path ($\lambda = 160$ g/cm²), deduced from the geometrical cross section for nuclear interactions in Pb and from the experimental cross section for the interactions in which penetrating showers are produced.²⁰

We do not attribute much quantitative significance to the present argument, nor insist that the interaction mean free path of the radiation producing low energy events is as small as that given by the geometrical cross section, yet we strongly believe that the interpretation of the absorption curve of the N -component must be made following this line.

A more accurate treatment of the problem should take into account the contribution to the development of the nuclear cascade of tertiary, quarternary, etc. interactions. However, it is easy to see that the more generations are involved, the more closely the curve c approaches to pure exponential with $\lambda_{obs} > \lambda$.

We think that this is the reason why the absorption curve in air of the N -component looks like a pure exponential curve, with a mean free path about twice that deduced from the geometrical cross section.

Performance of this experiment was made possible by a grant from the Research Corporation.

The facilities of the Echo Lake Inter-University High Altitude Laboratory were of invaluable help.

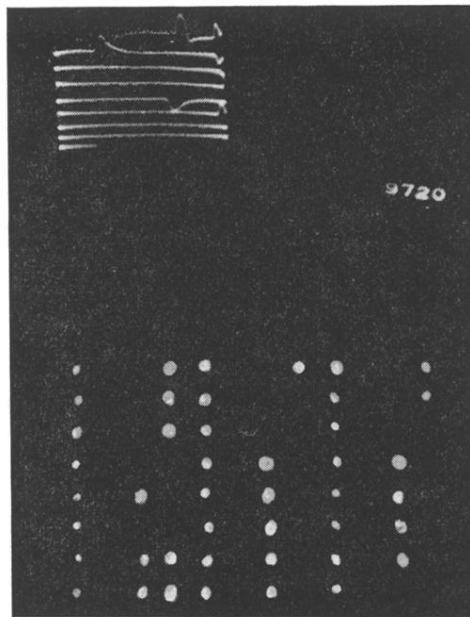
We wish to thank Professor K. Greisen and Professor H. Bethe for discussions and suggestions.

¹⁸ Bernardini, Cortini, and Manfredini, Phys. Rev. **76**, 1792 (1949).

¹⁹ E. P. George, Nature **162**, 333 (1948). E. P. George and A. C. Jason, Proc. Phys. Soc. London **A62**, 243 (1949). See reference 18.

²⁰ G. Cocconi, Phys. Rev. **76**, 984 (1949). See reference 12. K. Sittte, Phys. Rev. **78**, 714 (1950).

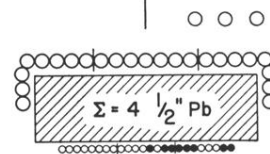
FIG. 3. Example of a picture (a) and a card (b) of a shower probably produced by a neutral primary. One neutron is required to trigger the sweep of the CRT, 7 neutron pulses are visible on the sweep. No neon bulbs are lit in columns 1, 2, and 3 of the hodoscope, which are connected to the counters in tray *a*. The bulbs in columns 4, 8, and 12 are always lit to provide fiducial marks. The bulbs in column 5, 6, and 7 are connected to tray *b*; 9, 10, and 11 to tray *c*; and 13, 14, and 15 to tray *d*.



(a)

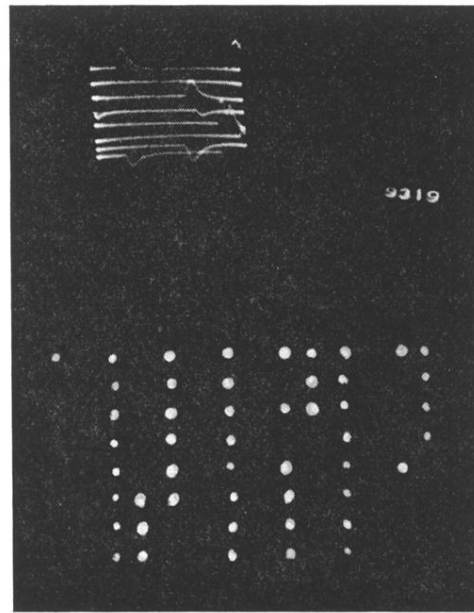
TOTAL NUMBER OF NEUTRONS: 8

UP	DOWN
16 μ sec	69 μ sec
27	113
43	185
238	



(b)

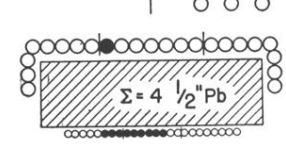
FIG. 4. Example of a picture (a) and a card (b) of a shower probably produced by an ionizing primary.



(a)

TOTAL NUMBER OF NEUTRONS: 11

UP	DOWN
2 μ sec	133 μ sec
12	158
112	284
205	300
207	
255	



(b)